AIP | Applied Physics Letters

Electronic and interface properties of polyfluorene films on GaN for hybrid optoelectronic applications

G. Itskos, X. Xristodoulou, E. Iliopoulos, S. Ladas, S. Kennou et al.

Citation: Appl. Phys. Lett. **102**, 063303 (2013); doi: 10.1063/1.4792211
View online: http://dx.doi.org/10.1063/1.4792211
View Table of Contents: http://apl.aip.org/resource/1/APPLAB/v102/i6
Published by the AIP Publishing LLC.

Electronic and interface properties of polyfluorene films on GaN for hybrid optoelectronic applications

G. Itskos,[1,a)] X. Xristodoulou,[1] E. Iliopoulos,[2,3] S. Ladas,[4] S. Kennou,[4] M. Neophytou,[5] and S. Choulis[5]
[1]*Experimental Condensed Matter Physics Laboratory, Physics Department, University of Cyprus, Nicosia 1678, Cyprus*
[2]*Institute of Electronic Structure and Laser (IESL), Foundation for Research and Technology-Hellas (FORTH), 71110 Heraklion, Greece*
[3]*Physics Department, University of Crete, 71003 Heraklion, Greece*
[4]*Department of Chemical Engineering, University of Patras, Patras GR-26504, Greece*
[5]*Molecular Electronics and Photonics Research Unit, Department of Mechanical Engineering and Materials Science and Engineering, Cyprus University of Technology, Limassol 3603, Cyprus*

(Received 21 November 2012; accepted 31 January 2013; published online 13 February 2013)

Electronic and interface properties of spin-coated poly(9,9-dioctylfluorenyl-2,7-diyl) (PFO) films on GaN have been investigated in terms of their potential for optoelectronic applications. The PFO/GaN interface was studied by photoemission spectroscopy showing a type-II energy alignment with band offsets suitable for efficient photocurrent generation. The light harvesting potential is further supported by fluorescence experiments that show evidence of photo-induced electron transfer from PFO to GaN. The impact of polymer film thickness was probed using emission anisotropy and ellipsometry, indicating the presence of an ordered planar phase of PFO. The study has implications to hybrid optoelectronic devices employing the two important materials. © *2013 American Institute of Physics*. [http://dx.doi.org/10.1063/1.4792211]

Heterogeneous structures of organic and inorganic semiconductors can employ the favorable properties of each class of materials to offer improved functionalities to optoelectronic devices.[1] The use of solution processing methods to deposit the organic component on the top surface of an inorganic semiconductor wafer adds to the ease of fabrication of planar hybrid structures and allows the monolithic incorporation of different semiconductors that are not necessarily lattice matched. This approach creates enormous possibilities of combining organic and epitaxial inorganic semiconductors into hybrid optoelectronic devices but also imposes the need for fundamental studies of the intermaterial interactions and the nature and disorder of the hybrid interface(s).

Assemblies of nitrides and organics for optoelectronic applications have been under investigation since the early stage development of GaN.[2,3] Efforts have mostly concentrated on light emission based on downconversion by the nitride to achieve white light,[2,4–6] multi-color microarrays,[7,8] and even polymer lasing.[9] Nitride-organic light harvesting have been more recently under investigation with demonstrations of photosensors[10,11] and solar cells.[12] Some of the most promising studies combined (Ga,In)N structures with polyfluorenes known for their high absorption coefficients and fluorescence quantum efficiencies.[13,14] Planar structures of the aforementioned materials have been employed to demonstrate efficient emission across the entire visible, coupled radiatively via downconversion[7,8] or non-radiatively via Forster resonant energy transfer (FRET).[15–17]

In both cases, intermaterial interactions are expected to be strongly affected by the heterointerface. Interfacial disorder and band alignment are also critical parameters for the performance of potential Polyfluorene/GaN junction devices such as those of Refs. 10–12 yet no relevant studies exist in the literature. Furthermore, some of the aforementioned structures employ surface quantum wells (QWs)[18] and ultrathin organic films, both of which have been scarcely employed in devices before and thus are rather unexplored.

We report on the investigation of spin-coated ultrathin to thin (~5–55 nm) films of the prototype polyfluorene homopolymer poly(9,9-dioctylfluorenyl-2,7-diyl) (PFO) deposited on GaN wafers and control fused silica and sapphire (Al_2O_3) substrates. A combination of optical spectroscopy, namely steady-state and time-resolved photoluminescence (PL) emission, excitation (PLE) and anisotropy experiments, and surface techniques such as X-ray and ultraviolet photoemission and ellipsometry have been employed to probe the electronic and interface properties of the hybrid structures.

Poly(9,9-dioctylfluorenyl-2,7-diyl) (PFO) end capped with N,N-Bis(4-methyl-phenyl)-4-aniline was purchased from American Dye Source Inc (ADS329BE). The material was diluted in a 1 mg/ml concentration in chlorobenzene. The solution was left stirring at 80 °C for more than one hour and was spin-coated on polar [0001] c-plane GaN, c-plane Al_2O_3 and fused silica (spectrosil B) substrates that have been cleaned by acetone and isopropyl alcohol. Apart from the cleaning, no other chemical treatment of the substrate surfaces was carried out. Rotational speeds of 3000–5000 rpm were used, followed by a 6000 rpm drying step, to achieve polymer films in the range of ~5 to 55 nm. Film thicknesses were measured with a Dectak Profilometer with accuracy of ±2 nm.

To probe the surface and interface characteristics of PFO on (0001) GaN, two samples, a reference pristine GaN and a hybrid structure composed of a 5 nm thin PFO on GaN were introduced to ultra-high vacuum conditions and characterized by X-ray and ultraviolet photoemission spectroscopy

a)Author to whom correspondence should be addressed. Electronic mail: itskos@ucy.ac.cy.

(XPS/UPS). Unmonochromatized Mg Ka line at 1253.6 eV and a hemispherical analyzer with multichannel detector, at a pass energy of 100 eV, were used in XPS measurements. For the UPS measurements, the HeI (21.22 eV) excitation line was employed. A negative bias of 12.28 V was applied to the sample during UPS measurements in order to separate sample and analyzer high binding energy cut-off and estimate the absolute work function value from the UPS spectra.

The XPS spectra show that only C, O, Ga, and N are present in both samples in the analysis depth (about 10 nm). In the reference sample C and O are due to atmosphere contamination. In the PFO/GaN sample, Ga and N are coming from the substrate since the PFO layer is thinner than the analysis depth. Oxygen is also due to contamination. Fig. 1 shows the UPS valence band spectrum of the reference GaN (top) and the hybrid PFO/GaN (bottom) sample. For the control GaN sample, the valence band (VB) edge obtained from the right part of the spectrum is determined at 2.1 eV from the Fermi level. The work function obtained from the high binding energy cutoff was estimated at 4.4 eV. From these values, an ionization energy ($IE = (E_{Vac} - E_{VB})$ of 6.5 ± 0.1 eV is estimated, where E_{Vac} is the vacuum energy. Considering an energy gap of $Eg = 3.4$ eV at room temperature, the electron affinity ($EA = E_{Vac} - E_{CB}$) is found equal to 3.1 ± 0.1 eV, in good agreement with values reported in the literature.[19,20] The energy state values measured indicate an n-type character of the GaN substrate.

The bottom part of Fig. 1 shows the valence band spectrum of the PFO/GaN sample. As the analysis depth of the UPS is of the order of 3 nm, the spectrum is mainly related to the PFO valence band where contributions from the phenyl back bone and the alkyl side chains exist. The HOMO onset is estimated at 1.5 eV from the Fermi level and the high binding energy cutoff at 4.1 eV. The peaks labeled A and B at ~2 eV and ~4 eV in the figure are attributed to the localized π states of the polymer backbone. Using the HOMO and energy cutoff values, the ionization potential is estimated at 5.6 ± 0.1 eV, in agreement with the literature.[21] From the experimental data, the energy level diagram at the interface is drawn in Fig. 2. The measurements confirm a type-II alignment with CB/LUMO and VB/HOMO band offsets of 0.4 and 0.6 eV, respectively. The CB/LUMO offset is comparable and slightly higher to measured values of the PFO exciton binding energy (~0.3 eV)[22] indicating an energy level alignment that can promote efficient photocurrent generation, as it allows for interfacial exciton dissociation via an electron transfer process to GaN while potentially minimizing electron thermal losses in the acceptor (GaN) material. Considering a Fermi level alignment of the two materials, evidenced by the absence of XPS peaks shifts in the two samples and supported by previous studies of the PFO interface with Au, ITO, and PEDOT:PSS (Ref. 23), the measurements indicate the formation of a small interface dipole of 0.3 ± 0.1 eV.

Steady-state and time-resolved PL emission and PLE were employed to investigate the influence of thickness and substrate type on the spectral and temporal characteristics of the PFO fluorescence. Steady-state PL was carried out using a 0.75 m spectrometer equipped with a CCD camera, excited either by the 355 nm line of the triple harmonic of a nanosecond pulsed Nd:YAG laser or a chopped (20 Hz) 375 nm laser diode. PLE was excited by an ozone-free 450 W Xenon lamp and monitored by a spectrophotometer equipped with a photomultiplier tube. Time-resolved PL was measured by a 0.35 m spectrometer-based, time-correlated single-photon counting (TCSPC) setup using a 375 nm ps laser diode. The system exhibits a time-resolution of 50 ps after reconvolution with the instrument response function.

Normalized PLE spectra (top) of identical 15 nm PFO films on GaN and Al_2O_3 are displayed on the left hand side of Fig. 3 (top). The PLE spectrum of the latter film contains a feature peaked at 400 nm, typical of PFO π-π^* transitions and qualitatively matches the film absorption spectrum. The excitation spectra of the GaN deposited film on the other hand, contain a structured, broad feature extending further into UV due to strong emissive contributions from the GaN band-edge states. This is supported by fluorescence experiments performed using photo-excitation above the GaN energy gap at 355 nm, that show significant enhancement of the polymer emission in GaN relative to films on sapphire or glass, due to radiative pumping by the underlying GaN layer.

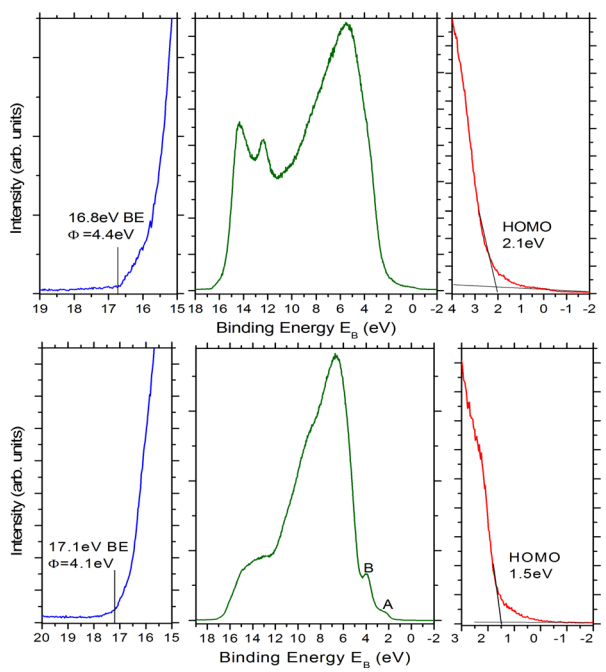

FIG. 1. UPS spectra of: GaN control (top) and PFO/GaN (bottom) samples. In magnification, the low energy part of the spectrum where the valence band edge is obtained from (right) and the high binding energy cutoff where the work function is obtained from (left), are shown.

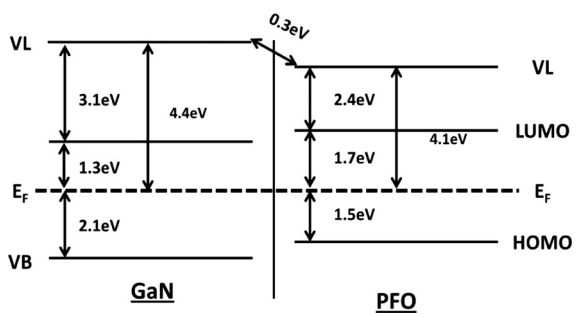

FIG. 2. Energy level diagram of the PFO/GaN interface obtained by UPS studies of pristine GaN and PFO/GaN samples.

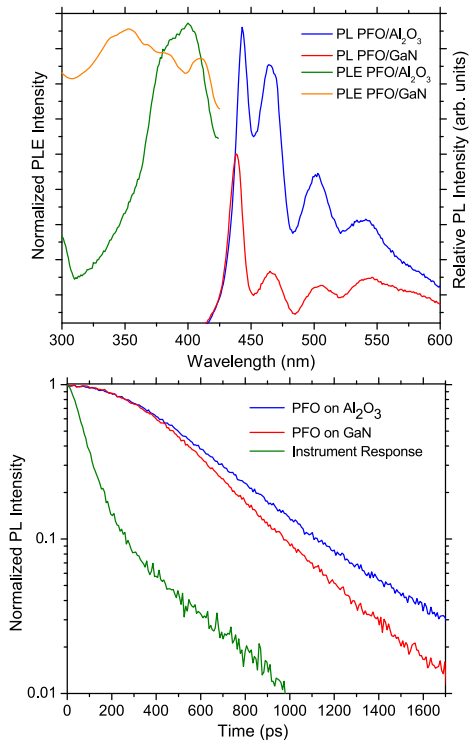

FIG. 3. PL (right) and PLE (left) spectra of 15 nm PFO films on GaN and Al_2O_3 (top). Normalized PL decays monitoring the 0-0 peak of PFO of the aforementioned samples in a logarithmic scale (bottom). The instrument response is also displayed.

However, the situation reverses under photoexcitation at 375 nm, below the GaN band-edge, where the PL emission intensity of sapphire deposited films is systematically higher than those deposited on GaN. The comparative PL spectra of the 15 nm films on the two types of substrates are shown on the right hand-side of Fig. 3 (top). Both films exhibit the characteristic singlet exciton PFO vibronic progression with the GaN deposited film showing a high intensity ratio of the 0-0 to the higher vibronic modes for reasons discussed later in the manuscript. Of interest here is that the integrated emission of PFO on GaN is quenched by a factor of ~2 relative to that of the film on sapphire. Overall, a consistent quenching of the PFO/GaN integrated emission by factors of ~1.25 to ~3 compared to films of equal thicknesses on sapphire, for thicknesses up to 55 nm, has been observed.

The quenching is also present at the dynamics of the polymer exciton emission. Fig. 3 (bottom) displays PL decays of the two 15 nm films on GaN and Al_2O_3 obtained by photoexcitation at 375 nm. The displayed traces are obtained when the temporal evolution of the 0-0 peak of the PFO emission was monitored. The two decays are to a good approximation mono-exponentials with time constants of ~445 ps and ~375 ps for the film on Al_2O_3 and GaN, respectively, i.e., a faster decay by ~20% is measured in the latter relative to the former film. Overall quenching of the PFO exciton lifetime in GaN deposited films relative to films on sapphire, by factors of ~10%–25% were measured, with higher quenching factors generally observed for thinner film comparisons.

The systematic appearance of steady-state and time-resolved fluorescence quenching in the films on GaN relative to those on Al_2O_3 are indicative of the presence of an additional exciton relaxation channel in the former films. We attribute the channel to photo-induced electron transfer processes from the PFO to GaN across the heterointerface. Such processes are energetically allowed by the measured band offsets as explained above, and are consistent with the observation of larger TR-PL quenching for thinner PFO films. Thinner films allow for a higher exciton dissociation probability on the PFO/GaN interface as the Frenkel exciton diffusion length of ~5 nm (Ref. 24) compares more favorably to the film thicknesses. Indicative values of the electron transfer times can be obtained by computing the decay rates of the films on GaN and Al_2O_3. In the example of the Fig. 3, the decay rates of the films on GaN and Al_2O_3 are ~2.67 ns^{-1} and ~2.25 ns^{-1}, respectively. The electron transfer rate can then be estimated by the difference of the two decay rates, namely, 2.67–2.25 $ns^{-1} = 0.42\ ns^{-1}$ from which an electron transfer time of ~2.4 ns is obtained. Overall electron transfer times from PFO to GaN of ~2–10 ns were obtained in the studied films using the described comparative TR-PL method. Higher electron transfer rates for polyfluorene/GaN device applications may be obtained by further studies that can investigate in detail the interfacial disorder and the influence of nitride surface termination, i.e., III-rich or N-rich growth and polarity, i.e., polar versus non-polar substrates,[11] on the GaN/PFO energy level alignment.

The impact of film thickness on the photophysics of PFO films on GaN, Al_2O_3, and glass substrates was also studied. Variable angle spectroscopic ellipsometry (VASE) measurements on thin (~15 nm) polyfluorene (PFO) films on fused silica (spectrosil B) substrates were performed. The measurements were taken in the spectral region of 300–1000 nm, for a range of incidence angles from 50° to 80°. The data were analyzed using a simple bilayer optical model (PFO/Glass), with the PFO dielectric function modeled by generalized oscillators[25] to ensure Kramers-Kronig consistency. The results of the PFO deduced dielectric function, expressed as refractive index n and extinction coefficient k, are shown in Fig. 4 (bottom).

The model assumes isotropic optical properties of the film taking into account the amorphous nature of the substrate. The assumption is supported by previous studies of PFO films on glass[26] and PL anisotropy measurements presented later in the manuscript that show small values of emission anisotropy in PFO films deposited in fused silica. In the top of Fig. 4, the measured ellipsometric angles for two incident angles are shown and compared to the simulated ones (red lines) based on the deduced PFO dielectric function. Compared to similar VASE measurements on thicker PFO films[26] (>100 nm), the ultrathin films of our studies exhibit increased oscillator strengths of the 0-0 vibronic and slightly higher values of the refractive index n and extinction coefficient k.

Support of the ellipsometry findings is provided by PL experiments. Comparative PL measurements show that thin films of thicknesses typically less than 25–30 nm deposited on either GaN or Al_2O_3 exhibited unusually strong emission and higher intensity ratios of the 0-0 to the higher vibronic modes. To further investigate the effect, a TR-PL study was carried out. The results of such a study for films on GaN substrates when monitoring the 0-0 vibronic mode are displayed on Fig. 5. A correlation between PFO exciton lifetime and film thickness is evident with thinner films showing a faster

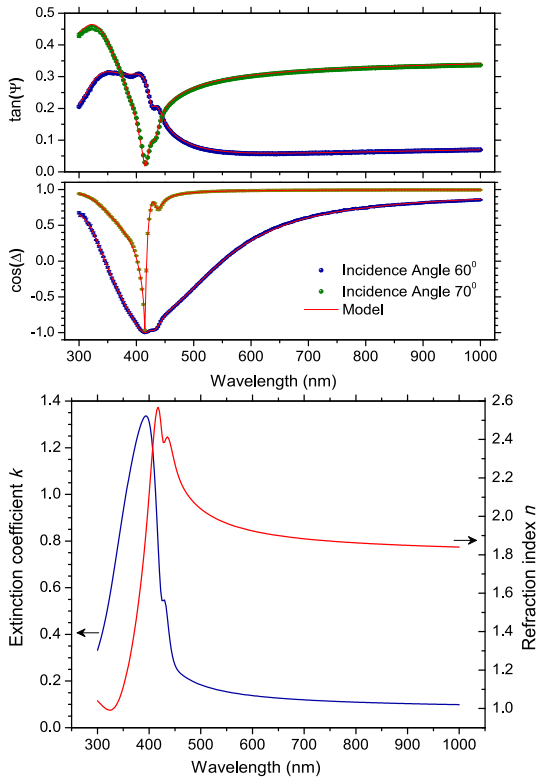

FIG. 4. Variable angle ellipsometry of a 15 nm PFO spin-coated on glass: Example of the fitted model to experimental data for incidence angles of 60 and 70 degrees (top). Derived complex dielectric function of PFO, expressed as refractive index *n* and extinction coefficient k (bottom).

decay. In particular, as the film thickness decreases from 55 to 10 nm, the decay constants decrease from ~400 to ~350 ps, respectively. A similar trend of decay lifetime versus thickness was also observed on PFO films on sapphire. The faster decays of thinner films can be predominantly attributed to higher fluorescence rates consistent with the strong emission they exhibit in the steady-state spectra.

To explore the origin of the effect, we performed time-resolved measurements of the photo-induced anisotropy on the films. The linearly polarized line of the pulsed 375 nm laser was used as the excitation, while the linear polarization of the emitted luminescence was analyzed by a Glan-Thomson polarizer, placed before the detecting spectrometer. The geometry employed is graphically displayed at the top of Fig. 6. The sample was excited at nearly normal incidence

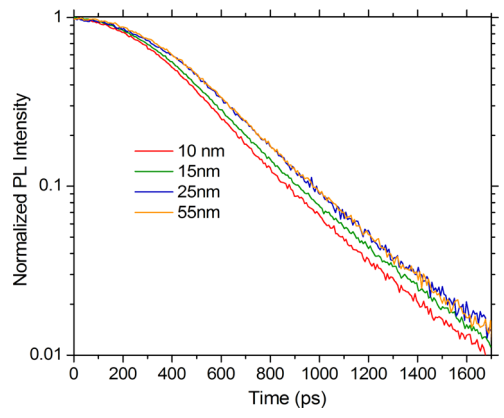

FIG. 5. Normalized PL decays of PFO films of different thicknesses (10–55 nm) on GaN obtained at the 0-0 vibronic peak of PFO.

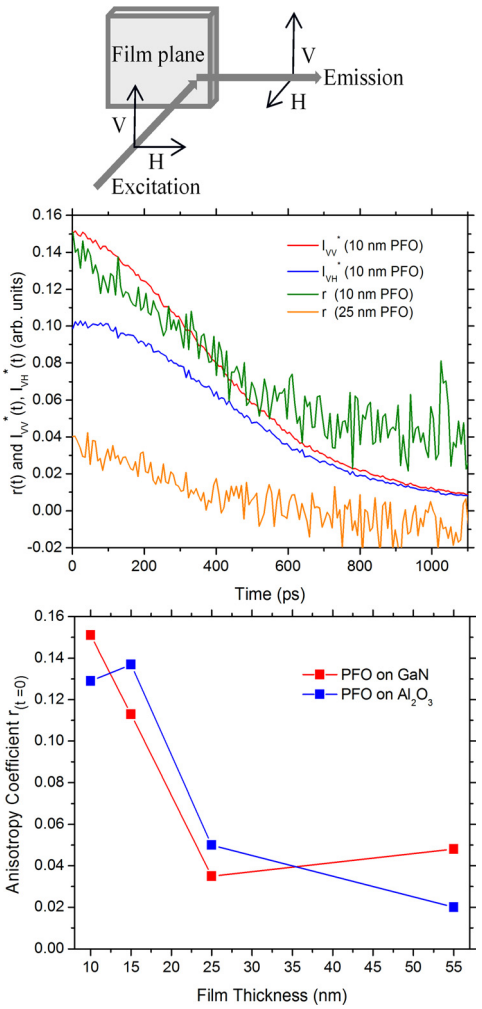

FIG. 6. I_{VV}^* (red) and I_{VH}^* (blue) decays and emission anisotropy coefficient r(t) (green) for a 10 nm PFO film on GaN and r(t) for a thicker 25 nm film on GaN (orange) (top). Anisotropy coefficient at t = 0 of different thickness PFO films on GaN and Al_2O_3 (bottom).

and the side-emission in the vicinity of the 0-0 PFO vibronic peak was spectrally and temporally resolved and detected. The polarization of the excitation and emission was selected between the vertical and horizontal directions defined on the display of Fig. 6. Experimentally four decays per sample were measured, defined by the indexes I_{VV}, I_{VH}, I_{HV}, and I_{HH}, where the first index denotes the polarization of the excitation and the second the polarization of the emission.

The emission anisotropy is typically quantified by the anisotropy coefficient defined as

$$r = \frac{I_{VV} - G*I_{VH}}{I_{VV} + 2*G*I_{VH}}, \quad (1)$$

where $G = \frac{I_{HV}}{I_{HH}}$ is the correction factor that accounts for the different sensitivity of the detection system to vertical and horizontal polarizations of light.

The temporal evolution of the emission anisotropy coefficient r(t) was recorded for four film thicknesses of ~10, 15, 25, and 55 nm on GaN and sapphire, a total of 8 samples. Fig. 6 (middle) shows the instrument corrected I_{VV}^* and I_{VH}^* decays (red and blue curves, respectively) and the calculated emission anisotropy coefficient r(t) (green curve) for the

10 nm PFO film on GaN. The coefficient exhibits a modest value of ~0.15 at t = 0, corresponding roughly to a 20% linear polarized emission, and decays to a good approximation mono-exponentially with a time constant of ~500 ps. The anisotropy coefficient does not decay to zero saturating at a value of 0.04. Time-integrated PL spectra show a steady-state anisotropy coefficient of 0.08, corresponding roughly to a linear polarized emission of the 0-0 PFO vibronic of ~12%. In the same graph r(t) for a thicker 25 nm PFO film on GaN is also displayed (orange curve). The anisotropy coefficient exhibits a significantly smaller value of ~0.04 at t = 0 and decays to zero within 400 ps, while time integrated spectra show a linear polarization of less than 5%.

The maximum (t = 0) value of the emission anisotropy of all studied films is summarized at the bottom of Fig. 6. A dependence of anisotropy on film thicknesses is evident on both GaN and Al_2O_3 deposited films, with significant higher values obtained for the ultrathin 10 and 15 nm films. Furthermore, the coefficient was found to decay slower for thinner films and saturates at small but non-zero values for the thin 10 and 15 nm films while for thicker films it decays to zero. In the geometry employed in our experiments, the data imply a preferential in-plane orientation of the transition dipole moments for thin films which in turn indicates that a fraction of the polymer chains in such films acquire a more rigid, planar conformation. Similar trends of the optical anisotropy of spin-coated films with thickness have been observed for other conjugated polymers indicating a polymer chain alignment parallel to the substrate.[27] In our case, the conformation in which the fluorene repeat units are planarized with respect to each other is known as β-phase.[13,14,28] Such a phase is usually induced by thermal treatment or solvent annealing, however, it is possible that at the very small thicknesses employed even unprocessed spin-casted films contain a fraction of β-chains. The assignment is supported by the findings of ellipsometry and time-resolved measurements that show enhanced optical constants and oscillator strength of the 0-0 vibronic which is a typical optical signature, among others, of the PFO β-phase. It is noted that non-zero but significant smaller emission anisotropy was measured on films of the same thickness on fused silica (amorphous) substrates indicating that the crystallinity and polarizability of the GaN and Al_2O_3 substrates affects the conformation of the overlaying PFO chains.

In summary, the PFO/GaN interface was investigated by photoemission experiments to obtain the energy band diagram of the two materials. Supported by PL studies that show evidence of photo-induced electron transfer from the PFO to GaN, the measurements indicate that the GaN/PFO interface can be exploited in sensor devices in which light harvesting occurs on the highly absorbing polyfluorene material with subsequent interfacial exciton dissociation and electron/hole transport on the inorganic/organic component, respectively. We have also investigated the effect of the thickness on the photophysics of PFO films deposited on crystalline (GaN, Al_2O_3) and amorphous (fused silica) substrates. At ultrathin films on the crystalline substrates, enhanced oscillator strengths and a preferential ordered planar chain conformation, most probably attributed to the β-phase of PFO, was found to exist. Such findings have implications to light emitting structures employing ultrathin polyfluorene films in nitrides such as those reported in FRET-coupled InGaN-polyfluorene hybrids.[8,15–17] A preferential alignment of the optical dipole moments of the polymer may result in an increased dipole-dipole interaction. The hypothesis is supported by a recent theoretical study[29] that shows that the FRET rate can be enhanced by up to a factor of two depending on the crystal orientation of the organic material.

G. Itskos, X. Xristodoulou, E. Iliopoulos, M. Neophytou and S. Choulis thank the Cyprus Research Promotion Foundation for financial support of the project via the infrastructure upgrade research Grant "ANABAΘMIΣH/0609/15."

[1]V. M. Agranovich, Yu. N. Gartstein, and M. Litinskaya, Chem. Rev. **111**, 5179 (2011).
[2]F. Hide, P. Kozodoy, S. P. DenBaars, and A. J. Heeger, Appl. Phys. Lett. **70**, 2664 (1997).
[3]J. O. McCaldin, Prog. Solid State Chem. **26**, 241 (1998).
[4]H.-F. Xiang, S.-C. Yu, C.-M. Che, and P. T. Lai, Appl. Phys. Lett. **83**, 1518 (2003).
[5]H.-J. Kim, J.-Y. Jin, Y.-S. Lee, S.-H. Lee, and C.-H. Hong, Chem. Phys. Lett. **431**, 341 (2006).
[6]I. O. Huyal, U. Koldemir, T. Ozel, H. V. Demir, and D. Tuncel, J. Mater. Chem. **18**, 3568 (2008).
[7]G. Heliotis, P. N. Stavrinou, D. D. C. Bradley, E. Gu, C. Griffin, C. W. Jeon, and M. D. Dawson, Appl. Phys. Lett. **87**, 103505 (2005).
[8]C. R. Belton, G. Itskos, G. Heliotis, P. N. Stavrinou, P. G. Lagoudakis, J. Lupton, S. Pereira, E. Gu, C. Griffin, B. Guilhabert, I. M. Watson, A. R. Mackintosh, R. A. Pethrick, J. Feldmann, R. Murray, M. D. Dawson, and D. D. C. Bradley, J. Phys. D: Appl. Phys. **41**, 094006 (2008).
[9]Y. Yang, G. A. Turnbull, and I. D. W. Samuel, Appl. Phys. Lett. **92**, 163306 (2008).
[10]H. Kim, Q. Zhang, Yoon-Kyu Song, A. Nurmikko, Q. Sun, and J. Han, Phys. Status Solidi C **6**, 593 (2009).
[11]H. Kim, Ze-Lei Guan, Q. Sun, A. Kahn, J. Han, and A. Nurmikko, J. Appl. Phys. **107**, 113707 (2010).
[12]N. Matsuki, Y. Irokawa, Y. Nakano, and M. Sumiya, Sol. Energy Mater Sol. Cells **95**, 284 (2011).
[13]U. Scherf and E. J. W. List, Adv. Mater. **14**, 477 (2002).
[14]R. Abbel, A. P. H. J. Schenning, and E. W. Meijer, J. Polym. Sci. A: Polym. Chem. **47**, 4215 (2009).
[15]G. Heliotis, G. Itskos, R. Murray, M. D. Dawson, I. M. Watson, and D. D. C. Bradley, Adv. Mater. **18**, 334 (2006).
[16]G. Itskos, G. Heliotis, P. G. Lagoudakis, J. Lupton, N. P. Barradas, E. Alves, S. Pereira, I. M. Watson, M. D. Dawson, J. Feldmann, R. Murray, and D. D. C. Bradley, Phys. Rev. B **76**, 035344 (2007).
[17]G. Itskos, C. R. Belton, G. Heliotis, I. M. Watson, M. D. Dawson, R. Murray, and D. D. C. Bradley, Nanotechnology **20**, 275207 (2009).
[18]A. Othonos, G. Itskos, D. D. C. Bradley, M. D. Dawson, and I. M. Watson, Appl. Phys. Lett. **94**, 203102 (2009).
[19]C. I. Wu, A. Kahn, N. Taskar, D. Dorman, and D. Gallagher, J. Appl. Phys. **83**, 4249 (1998).
[20]T. E. Cook, Jr., C. C. Fulton, W. J. Mecouch, K. M. Tracy, R. F. Davis, E. H. Hurt, G. Lucovsky, and R. J. Nemanich, J. Appl. Phys. **93**, 3995 (2003).
[21]L. S. Liao, M. K. Fung, L. F. Cheng, C. S. Lee, S. T. Lee, M. Inbasekaran, E. P. Woo, and W. W. Wu, Appl. Phys. Lett. **77**, 3191 (2000).
[22]S. F. Alvarado, P. F. Seidler, D. G. Lidzey, and D. D. C. Bradley, Phys. Rev. Lett. **81**, 1082 (1998).
[23]J. Hwang and A. Khan, J. Appl. Phys. **97**, 103705 (2005)
[24]M. Stoessel, G. Wittmann, J. Staudigel, F. Steuber, J. Blässing, W. Roth, H. Klausmann, W. Rogler, J. Simmerer, A. Winnacker, M. Inbasekaran, and E. P. Woo, J. Appl. Phys. **87**, 4467 (2000).
[25]B. Johs, C. M. Herzinger, J. H. Dinan, A. Cornfeld, and J. D. Benson, Thin Solid Films **313–314**, 137 (1998).
[26]M. Campoy-Quiles, G. Heliotis, R. Xia, M. Ariu, M. Pintani, P. Etchegoin, and D. D. C. Bradley, Adv. Funct. Mater. **15**, 925 (2005).
[27]U. Zhokhavets, G. Gobsch, H. Hoppe, and N. S. Sariciftci, Thin Solid Films **451–452**, 69 (2004).
[28]A. J. Cadby, P. A. Lane, H. Mellor, S. J. Martin, M. Grell, C. Giebeler, D. D. C. Bradley, M. Wohlgenannt, C. An, and Z. V. Vardeny, Phys. Rev. B **62**, 15604 (2000).
[29]S. Kawka and G. C. La Rocca, Phys. Rev. B **85**, 115305 (2012).